HHS Public Access

Author manuscript

Toxicol Lett. Author manuscript; available in PMC 2022 June 18.

Published in final edited form as:

Toxicol Lett. 2021 April 01; 340: 33–42. doi:10.1016/j.toxlet.2021.01.005.

Glutathione is a potential therapeutic target for acrolein toxicity in the cornea

Suneel Gupta[a,b],

Sabeeh Kamil[a,b],

Prashant R. Sinha[a,b],

Jason T. Rodier[a,c],

Shyam S. Chaurasia[a,b],

Rajiv R. Mohan[a,b,c,*]

[a] Harry S. Truman Memorial Veterans' Hospital, Columbia, MO, United States

[b] One-Health Vision Research Program, Department of Veterinary Medicine & Surgery and Biomedical Sciences, College of Veterinary Medicine, University of Missouri, Columbia, MO, United States

[c] Mason Eye Institute, School of Medicine, University of Missouri, Columbia, MO, United States

Abstract

Toxic and volatile chemicals are widely used in household products and previously used as warfare agents, causing a public health threat worldwide. This study aimed to evaluate the extent of injury and mechanisms of acrolein toxicity in the cornea. Primary human corneal stromal fibroblasts cultures (hCSFs) from human donor cornea were cultured and exposed to acrolein toxicity with −/+ N-acetylcysteine (NAC) to study the mode of action in the presence of Buthionine sulphoximine (BSO). PrestoBlue and MTT assays were used to optimize acrolein, NAC, and BSO doses for hCSFs. Cell-based assays and qRT-PCR analyses were performed to understand the acrolein toxicity and mechanisms. Acrolein exposure leads to an increased reactive oxygen species (ROS), compromised glutathione (GSH) levels, and mitochondrial dysfunction. The TUNEL and caspase assays showed that acrolein caused cell death in hCSFs. These deleterious effects can be mitigated using NAC in hCSFs, suggesting that GSH can be a potential target for acrolein toxicity in the cornea.

Graphical Abstract

* Corresponding author at: Ophthalmology and Molecular Medicine, University of Missouri, 1600 E. Rollins St, Columbia, MO, 65211, United States. mohanr@health.missouri.edu (R.R. Mohan).

Authors contributions

S.G. performed experiments, data collection, statistical analysis and prepared the draft of the manuscript; S.K. assisted with draft preparation, P.R.S. assisted with immunofluorescence and qRT-PCR studies; J.T.R. assisted in data review and manuscript draft; S.S.C. provided important feedback and assisted in manuscript improvement and R.R.M. conceived the idea, supervised experiments, arranged for resources, made critical improvents and finalized the manuscript.

Declaration of Competing Interest

The authors report no declarations of interest.

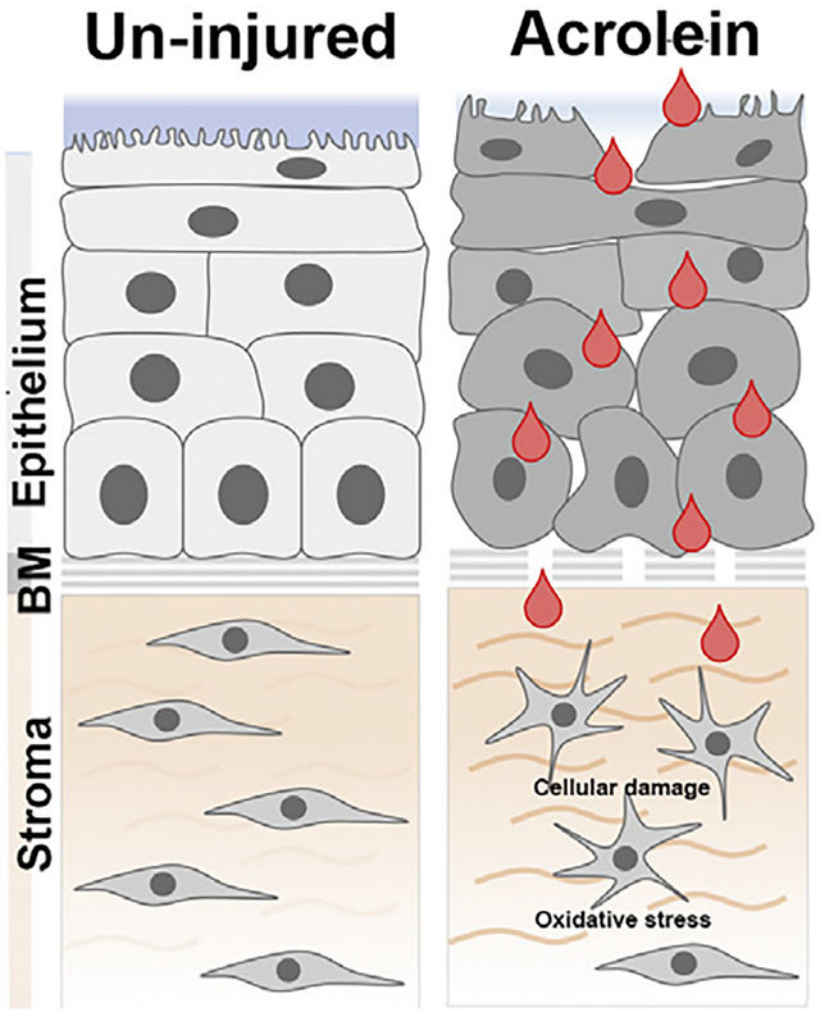

Keywords

Acrolein; Human corneal fibroblasts (hCSFs); Reactive oxygen species (ROS); Glutathione (GSH); Lipid peroxide (LPO); N-acetyl cysteine (NAC)

1. Introduction

Acrolein is a volatile organic compound with a sweet, pungent odor. It is used as a biocide in agriculture and as an intermediate to synthesize chemicals in several industries. The United States produces about 500 million pounds of acrolein annually (Ashizawa et al., 2007). Acrolein is also released into the environment as a pollutant from the fossil fuels, tobacco, and plastics. It can be formed when animal and vegetable oils are heated to high temperatures. Acrolein was also previously used as a warfare agent (“papite’) in World War I (Ghilarducci and Tjeerdema, 1995), posing a future global threat.

Acrolein exposure produces deleterious effects on various organs, including the eye (Ashizawa et al., 2007). Acrolein exposure to the eye in the war zone causes an immediate

response in eye closure, produces irritation, and lacrimation incapacitating the opponents in a battlefield (Claeson and Lind, 2016; Dachir et al., 2015). Depending upon the dose and duration, acrolein exposure may also produce corneal erosions, inflammation in the anterior chamber, and corneal neovascularization. In the long term, it can also cause limbal stem cell deficiency (Dachir et al., 2015; Gupta et al., 2020). Short-term treatment with local anesthetic and antiinflammatory drugs may prevent acute incapacitation from acrolein exposure to the cornea (Dachir et al., 2015). Currently, we do not have a definitive cure for acrolein toxicity primarily because of the unknown molecular mechanisms driving acrolein toxicity in the cornea.

Acrolein uses diverse molecular mechanisms to exert its toxic effects in tissues and organs. These mechanisms include oxidative stress, glutathione (GSH) depletion, mitochondrial damage, membrane disruption, protein adduction, DNA adduction, and endoplasmic reticulum stress. There is no single overarching pathway that integrates acrolein toxicity in various tissues (Moghe et al., 2015). In the eye, acrolein exposure produces cytotoxicity in retinal epithelial cells by increasing oxidative stress (Jia et al., 2007). Previous report has suggested that acrolein induced oxidative stress can be countered by increasing the endogenous GSH antioxidant index in lung fibroblast (Jia et al., 2009) to maintain the tissue homeostasis. However, molecular mechanisms of acrolein toxicity in the cornea are mostly unknown.

In this study, we exposed the primary cultures of human corneal stromal fibroblasts (hCSFs) generated from donor human corneas to acrolein and studied the effects on cytotoxicity and oxidative stress *in vitro*. We hypothesize that acrolein exposure increased oxidative stress, depletes glutathione, and compromises mitrochondrial function causing cell death in the hCSFs, which can be mitigated using N-acetylcysteine (NAC), known for its role in glutathione maintenance and metabolism.

2. Materials and methods

2.1. Chemicals and reagents

Acrolein, obtained from ULTRA Scientific Inc. (RCC-150, Thermo Fisher, Grand Island, NY, USA), was used to evaluate the toxic effects on hCSFs.

2.2. Primary cell cultures

The primary cultures of human corneal stromal fibroblasts (hCSFs) were generated from human donor corneas, procured from the Saving Sight (Kansas City, MO) using methods described earlier (Sharma et al., 2012). In brief, corneal buttons were sliced into pieces after scraping epithelium and endothelium and placed in a cell culture dish. They were maintained with minimal essential medium (MEM) supplemented with 10 % fetal bovine serum and incubated at 37 °C in a humidified chamber with 5% CO_2. The hCSFs of passage 4–6 were used for all *in vitro* experiments.

2.3. Cellular viability assays

2.3.1. MTT assay—The cellular viability was determined with MTT assay (3-(4,5-dimethylthiazol-2-yl)-2,5-diphenyltetrazolium bromide) using the CellTiter 96® Non-Radioactive Cell Proliferation Assay kit (Promega Corporation, Madison, WI, USA) following the manufacturer's protocol and as reported earlier (Gupta et al., 2011). In brief, the hCSFs were seeded in 96 well plates at a density of 5000 cells per well and incubated overnight at 37 °C in a humidified chamber with 5% CO_2. The fresh stock solutions of acrolein, NAC, and BSO were diluted in DMEM to the desired final concentrations immediately before every experiment. After the exposure of compounds, 15 μL of the MTT dye solution was added into each well. Plates were incubated at 37 °C in a CO_2 incubator for 4 h followed by the addition of 100 μL Solubilization Solution (Stop Mix). After one hour of incubation, optical density was measured at 570 nm using an Epoch BioTek plate reader (BioTek Instruments, VT, USA). Results were expressed as a reduction in cell viability with respect to the control (CTL) group treated with DMEM.

2.3.2. PrestoBlue assay—The cellular viability was also determined using the PrestoBlue cell viability reagents assay kit (Life Technologies, USA) following vendor instructions and as reported earlier (Lim et al., 2016). This cell permeable resazurin-based colorimetric method is a cell viability indicator that measures the reducing power of living cells to estimate the proliferation of cells quantitatively. In brief, the hCSFs were seeded in 96 well plates at a density of 5000 cells per well and incubated overnight at 37 °C in a humidified chamber with 5% CO_2. The fresh stock solutions of acrolein were diluted in DMEM to the desired final concentrations immediately before every experiment. After exposure of the compound, 20 μL of the 10x cell viability reagent was added to each well, and plates were incubated at 37 °C. After 10 min, the fluorescence was recorded at the excitation wavelength of 560 nm and an emission wavelength of 590 nm using an Epoch BioTek Synergy H4 Hybrid reader (BioTek Instruments, VT, USA). Results were expressed as a reduction in cell viability with respect to the control (CTL) group treated with DMEM.

2.4. Reactive oxygen species (ROS) assay

The levels of intracellular reactive oxygen species (ROS) in hCSFs were recorded qualitative and quantified using OxiSelect™ Intracellular ROS assay kit (Cell Biolabs, Inc, CA, USA) following the manufacturer's guidelines and as reported previously (Rodier et al., 2019). In brief, the hCSFs were seeded in 96 well plates at a density of 5000 cells per well and incubated overnight at 37 °C in a humidified chamber with 5% CO2. The cells were treated with 100 μL of 2′, 7′-Dichlorodihydrofluorescin diacetates (DCFH-DA) for 30 min at 37 °C. Intracellular ROS production leads to rapid oxidization of DCFH to highly fluorescent 2′, 7′-Dichlorodihydrofluorescein (DCF). After washing with PBS, cells were treated with different concentrations of evaluating compounds for 4 h. For qualitative analysis, the hCSFs were observed under a fluorescence microscope (Leica, DMI4000B, Leica Microsystems Inc., Buffalo Grove, IL, USA) equipped with a digital camera (SpotCam RT KE, Diagnostic Instruments Inc., Sterling Heights, MI, USA). For quantitative analysis, the cells were treated with 100 μL of lysis buffer, and the developed fluorescence intensity (proportional to the intracellular ROS) was measured at the excitation wavelength of 480 nm and the

emission wavelength of 530 nm using Epoch BioTek Synergy H4 Hybrid reader (BioTek Instruments, VT, USA).

2.5. Lipid peroxidation (LPO) assay

Lipid peroxidation (LPO) in hCSFs was quantified using Lipid peroxidation assay kit (Cayman Chemicals, Inc, MI, USA) following the manufacturer's guidelines. This assay measures the hydroperoxides, which converts ferrous ions to ferric ions. The resulting ferric ions are detected using thiocyanate ion as a chromogen. In brief, the hCSFs were seeded in 6-well plates at a density of 7.5×10^4 cells per well and incubated overnight at 37 °C in a humidified chamber with 5% CO_2. After 70 % confluency of hCSFs, the cultures were treated with different concentrations of evaluating compounds for 4 h. The exposed culture lysates were prepared according to the vendor instructions. For LPO analysis, experimental sample extracts (90 μL) were mixed with and FTS reagent 1 and FTS reagent 2 (100 μL). The 10 μL of freshly prepared chromogen solution was added, and plates were incubated at room temperature for 5 min. The absorbance of the resulting product was measured at 500 nm using an Epoch BioTek plate reader (BioTek Instruments, VT, USA), and hydroperoxide concentration in samples was calculated against the lipid hydroperoxide standard.

2.6. Glutathione (GSH) assay

Total glutathione (GSH) in hCSFs was quantified with the OxiSelect™ Total Glutathione (GSSG/GSH) assay kit (Cell Biolabs, Inc, CA, USA) following the manufacturer's guidelines. In brief, the hCSFs were seeded in 6-well plates at a density of 7.5×10^4 cells per well and incubated overnight at 37 °C in an incubator with 5% CO_2. After 70 % confluency of hCSFs, the cultures were treated with different concentrations of evaluating compounds for 4 h. The cells were detached by trypsinization, and the lysate was prepared according to the vendor instructions. For glutathione analysis, 25 μL of 1X glutathione reductase and 25 μL of 1X NADPH solution was mixed with 100 μL of samples. After that, 50 μL of 1X chromogen were added to the reaction mixture, and absorbance was measured at 405 nm using an Epoch BioTek plate reader (BioTek Instruments, VT, USA).

2.7. Mitochondrial membrane potential (ΔΨm)

Mitochondrial membrane potential (ΔΨm) in hCSFs was measured using the live Mitochondria tracker dye (MitoTracker™ Deep Red; Invitrogen, Molecular Probes Inc., OR, USA) following the vendor guidelines. In general, the cell-permeant MitoTracker probes contain a mildly thiol-reactive chloromethyl moiety for labeling mitochondria. The dye passively diffuses across the plasma membrane and accumulates in the active mitochondria in cells. The intake of the dye in the mitochondria is dependent upon the mitochondrial membrane potential (ΔΨm). In brief, the hCSFs were seeded in 6-well plates at a density of 7.5×10^4 cells per well and incubated overnight at 37 °C in a humidified chamber containing 5% CO_2. After 70 % confluency of hCSFs, the cultures were treated with different concentrations of evaluating compounds for 4 h. The MitoTracker dye (100 nM) was added to the exposed cultures. After 30 min, the alteration in membrane potential (ΔΨm) and degradation pattern was observed under fluorescence microscope (Leica, DMI4000B, Leica Microsystems Inc., Buffalo Grove, IL, USA) equipped with a digital camera (SpotCam RT KE, Diagnostic Instruments Inc., Sterling Heights, MI, USA).

2.8. Caspase 3/7 apoptosis assay

Caspase 3/7 1activitywas measured using Caspase-Glo® assay system (Promega, WI, USA) following the manufacturer's guidelines. The Caspase-Glo® 3/7 assay provides a pro-luminescent caspase-3/7 DEVD-aminoluciferin substrate and a thermostable luciferase in a reagent optimized for caspase-3/7 activity. The addition of this assay reagent to the cells liberates free aminoluciferin, which is consumed by the luciferase, generating a "glow-type" luminescent signal that is proportional to the caspase-3/7 activity. In brief, the hCSFs were seeded in 96 well plates at a density of 5000 cells per well and incubated overnight at 37 °C in an incubator with 5% CO_2. The cultures were treated with different concentrations of evaluating compounds for 4 h. For caspase activity, 100 μL of assay reagent was mixed with an equal volume of the samples (100 μL) and incubated at room temperature. After 3 h, luminescence was measured using BioTek Synergy H4 Hybrid reader (BioTek Instruments, VT, USA).

2.9. TUNEL assay

The cellular toxicity after acrolein exposure was determined in hCSFs with the TUNEL (Terminal deoxynucleotidyl transferase dUTP nick end labeling) assay (ApopTag; Millipore, Temecula, CA, USA) following the manufacturer's guidelines and as reported earlier (Gupta et al., 2017). This assay modifies DNA utilizing terminal deoxynucleotidyl transferase (TdT) to detect positive cells undergoing apoptosis. In brief, the hCSFs were seeded in 6-well plates at a density of 7.5×10^4 cells per well and incubated overnight at 37 °C in a humidified chamber containing 5% CO_2. After 70% confluency of hCSFs, the cultures were treated with different concentrations of evaluating compounds for 4 h. For TUNEL assay, cells were fixed in 1% paraformaldehyde for 10 min. Rhodamine-conjugated apoptotic cells (red) and 4′, 6-diamidine-2′-phenylindole dihydrochloride (DAPI)–stained nuclei (blue) were viewed and photographed with a fluorescence microscope (Leica, DMI4000B, Leica Microsystems Inc., Buffalo Grove, IL, USA) fitted with a digital camera system (SpotCamRT KE; Diagnostic Instruments, Sterling Heights, MI, USA). DAPI-stained nuclei and TUNEL-positive cells in untreated and treated tissues were quantified at 200X and 400X magnification in six randomly selected non-overlapping areas, as previously reported (Gupta et al., 2017).

2.10. qRT-PCR analysis

The relative changes in mRNA of hCSFs under different conditions were evaluated using quantitative real-time reverse transcription PCR (qRT-PCR) using QuantStudio 6 Flex™ Real-Time PCR System (Applied Biosystems, Carlsbad, CA). Total RNA was extracted from experimental hCSFs using the RNeasy Mini kit (Qiagen, Valencia, CA). 2 μg RNA was used for cDNA conversion using commercial reverse transcription system (Promega, Madison, WI) as reported earlier (Gupta et al., 2018). The changes in the mRNA expression of GPx4 (Glutathione Peroxidase 4), BAD (Bcl2-associated agonist of cell death and BAX (Bcl2-like protein 4) were studied. A 20 μL qPCR reaction mixture contained 2 μL of cDNA, 2 μL of 200 nM forward primer, 2 μL of 200 nM reverse primer, 10 μL of 2X SYBR green supermix (Bio-Rad Laboratories, Hercules, CA), and 4 μL of RNAse/DNAse free water. The qRT-PCR was run at universal cycle conditions, including initial denaturation at

95 °C for 10 min, and 40 cycles of denaturation at 95 °C for 15 s, annealing, and extension at 60 °C for 60 s. Primer sequences of the genes were mentioned in Table 1. Glyceraldehyde 3-phosphate dehydrogenase (GAPDH) was used as the housekeeping gene. The relative mRNA expression was calculated using the $2^{-\Delta\Delta Ct}$ method and reported as relative fold change with respect to the corresponding control values.

2.11. Statistical analysis

All experiments were conducted independently three times using samples in triplicates. The results were expressed as the fold/percentage changes with respect to the non-acrolein exposed control (CTL) group. The results were presented as mean ± SEM. GraphPad Prism 6.0 (GraphPad Software, La Jolla, CA) software was used for statistical analysis. Studen's *t*-test and one-way analysis of variance (ANOVA) with Bonferroni post hoc test were used for statistical analysis. $p \leq 0.05$ was considered significant.

3. Results

3.1. Acrolein exposure to hCSFs decreased cell viability in a dose-dependent manner

In vitro cell viability assays were used for the dose optimization of acrolein toxicity in the hCSFs. A previous study suggests that *in vitro* IC_{50} correlates with the *in vivo* LD_{50} in most cytotoxicity prediction models (National Academies of Sciences, 2015). To evaluate the toxic dose of acrolein in hCSFs, cultures were exposed to 10, 25, 50, 75, 100, 125, 150 μM of acrolein for 4 h. Cellular viability was assessed using MTT and PrestoBlue assays, and hCSFs were monitored *via* live phase-contrast microscopy (Fig. 1). Both the MTT- (Fig. 1A) and PrestoBlue (Fig. 1B) assays showed a similar toxicity pattern of acrolein exposure in hCSFs. The *in vitro* IC_{50} of acrolein was found 98.67 μM (Fig. 1C). Also, acrolein exposure affected the cellular viability of hCSFs in a dose-dependent manner as seen in the phase-contrast live biomicroscopy images (Fig. 1D–K). Acrolein exposure at the dose of 100 μM for 4 h caused 50% cell death of hCSFs and used for all the experiments.

3.2. Acrolein increased oxidative stress and lipid peroxides in hCSFs

Oxidative stress has been implicated in acrolein toxicity to the retinal, respiratory, renal, cardiovascular, and neural tissues (Moghe et al., 2015). Oxidative stress in hCSFs exposed to acrolein was assessed by intracellular ROS assay (Fig. 2). Live cell imaging showed a substantive increase in ROS (depicted by the intensity of red color that corroborated by more intracellular production of 2′,7′-dichlorodihydrofluorescein (DCF) fluorescence in hCSFs after acrolein exposure (Fig. 2B and D) compared to the untreated control group (Fig. 2A and C). Acrolein exposure in hCSFs significantly increased the generation of ROS (6.94 ± 0.32 -fold) in hCSFs ($p < 0.0001$) compared to the control group (Fig. 2E). ROS can oxidize cellular molecules like lipids associated with the plasma membranes or membranes of vital organelles like mitochondria. Also, we found that acrolein exposure to hCSFs caused a significant increase (4.06 ± 0.33 -fold, $p < 0.0001$) in LPO (Fig. 2F).

3.3. Acrolein reduced Glutathione indices in hCSFs

Glutathione (GSH) is the major intracellular antioxidant in the cells, and acrolein has been known to adversely affect GSH levels in the brain and lung cells (Shah et al., 2015).

In hCSFs, we found that acrolein exposure reduced the GSH levels by 34.7 ± 2.65 % with respect to the control group ($p < 0.001$, Fig. 3B). Next, we measured an antioxidant enzyme, Glutathione peroxidase 4 (GPx4), which unlike other GPxs, plays a vital role in the oxidative homeostasis of the cornea (Sakai et al., 2016; Uchida et al., 2017) and has a unique ability to reduce lipid peroxides within the membranes (Brigelius-Flohé and Maiorino, 2013; Yang et al., 2014). We measured the changes in expression of GPx4 after acrolein exposure by qRT-PCR. The expression of GPx4 was 0.44 ± 0.06 folds less in acrolein exposed hCSFs compared to the control group (Fig. 3C). Acrolein exposure reduced the antioxidant enzymes in hCSFs, which might contribute to the exacerbation of oxidative stress.

To further study the role of acrolein-mediated damage to the cellular glutathione, buthionine sulfoximine (BSO), a selective inhibitor of glutathione synthesis, was used to determine the potentiation of cellular toxicity caused by acrolein in hCSFs. The optimal dose of BSO in hCSFs was determined by MTT assay (Fig. 3A), and 100 μM dose of BSO was used. A combined exposure of BSO and acrolein decreased the glutathione and GPx4 ($p < 0.001$) levels. The cytotoxicity of acrolein in hCSFs may be primarily because of reduced levels of glutathione in hCSFs.

3.4. Acrolein exposure depolarized mitochondrial membrane and increased mitochondrial membrane permeability

Changes in mitochondrial membrane potential ($\Delta\Psi m$) are considered sensitive markers of cellular injury in acute exposures to toxins (National Academies of Sciences, 2015). We measured the mitochondrial membrane potential ($\Delta\Psi m$) using the MitoTracker™ Deep Red dye (Fig. 4). The intake of the MitoTracker™ Deep Red dye is dependent upon the potential across the mitochondrial membrane. Depolarization of mitochondria reduces the intake of MitoTracker™ Deep Red dye (Xiao et al., 2016). Acrolein exposed hCSFs had lesser uptake of this dye as compare to non-acrolein exposed hCSFs (Fig. 4A & B). The relative fluorescence unit (RFU) in the acrolein exposed hCSFs had a significant reduction of 49.5 ± 2.32 % ($p < 0.001$) with respect to the non-acrolein exposed hCSFs (Fig. 4C).

Acrolein exposure caused the depolarization of mitochondria in hCSFs. Mitochondrial membrane potential itself generates ROS, and mitochondrial depolarization may be a protective response in the case of acrolein induced oxidative stress unless accompanied by increased mitochondrial membrane permeability (Zorova et al., 2018). To determine if acrolein exposure also increased the mitochondrial permeability, we measured the expression of BAD and BAX genes (Fig. 4D & E). Acrolein exposed hCSFs showed increased expression of BAD gene (1.5±0.18 -fold; $p < 0.001$) and BAX gene (1.3±0.18 -fold; $p < 0.01$). This increased permeability in the presence of depolarized mitochondrial membrane may contribute to cytotoxic effects of acrolein in hCSFs.

3.5. Acrolein exposure triggered cell death in hCSFs via apoptosis

Additionally, increased permeability of mitochondria may release cytochrome C and may culminate in cellular death via apoptosis and activation of caspases 3/7 activity. Hence, we studied cell death with TUNEL assay and the activity of caspase 3/7 (Fig. 5). Acrolein exposed group showed more TUNEL positive cells as compared to the non-acrolein exposed

(CTL) group (Fig. 5A & B). Acrolein exposed hCSFs had 2.49±0.12 fold ($p < 0.001$) higher activity of caspase 3/7 (Fig. 5C) with respect to the non-acrolein exposed control.

3.6. Protective effects of NAC against acrolein exposure

We wanted to test if acrolein targets GSH and therapies specific to mitigate GSH can have a protective effect against acrolein exposure in hCSFs. We chose NAC as it is safe and known antidote for GSH deficiency indicated in several medical conditions (Salamon et al., 2019).

3.6.1. Cytoprotective effects of NAC against acrolein exposure in hCSFs—

The optimal safe dose of NAC for hCSFs was determined using the MTT assay. NAC had no effect on cellular viability of hCSFs at the dose of 0.1, 0.25, 0.5, 0.75 and 1.0 mM (Fig. 6 A). NAC at the dose of 1.0 mM was used to in the subsequent studies in hCSFs.

Phase-contrast live microscopy was used to assess the cytoprotective effects of NAC (Fig. 6). NAC alone did not affect the viability of hCSFs as compare to control hCSFs (Fig. 6B & C). NAC restored the cellular morphology and hence reduced the adverse effects of acrolein exposure on cellular viability of hCSFs as compare to acrolein exposed hCSFs (Fig. 6D & E).

3.6.2. Antioxidant effects of NAC against acrolein exposure in hCSFs—

Acrolein exposure increased oxidative stress and reduced the levels of glutathione in hCSFs. Antioxidant effects of NAC were studied with ROS assay, LPO assay, and measuring GSH content (Fig. 7). Treatment with NAC significantly decreased the generation of ROS and lipid hydroperoxides (Fig. 7A & B; $p < 0.001$) and mitigated the loss of GSH observed in the acrolein exposed hCSFs (Fig. 7C; $p < 0.001$).

3.6.3. Anti-apoptotic effects of NAC against acrolein exposure in hCSFs—

Acrolein exposure was found to depolarize the mitochondrial membrane, increase its permeability, and caused cell death via caspases 3/7 pathway. NAC treatment to hCSFs exposed to acrolein reduced the extent of mitochondrial depolarization (Fig. 8C & D), which could be due to the reduced generation of ROS and restoration of GSH levels in hCSFs. While in similar manner, no changes were noticed in uptake of MitoTracker™ Deep Red dye in NAC alone as compare to non exposed control hCSFs (Fig. 8A & B). The relative fluorescence unit (RFU) in the acrolein exposed hCSFs had a significant reduction of dye uptake with respect to the non-acrolein exposed hCSFs, while NAC treatment rescued the acolein induced mitochondrial damage (Fig. 8E; $p< 0.001$). Treatment of acrolein exposed hCSFs with NAC also reduced the activity of caspase 3/7 (Fig. 8F; $p < 0.001$) thus preventing the apoptosis of hCSFs caused by acrolein exposure.

4. Discussion

Exposure to acrolein, a volatile aldehyde, causes pathological morbidity in a time- and dose-dependent manner (Moghe et al., 2015) in a variety of tissues and organs, including the eye, skin and lungs. In the eye, toxic effects of acrolein can be mild symptoms such as pain, irritation, lacrimation, and eyelid-swelling (Claeson and Lind, 2016; Dachir et al., 2015) to severe pathology, causing corneal burns and vision loss. Recently, we reported *in*

vivo acrolein exposure to the rabbit eye caused significant damage to the corneal stromal layer caused by the infiltration of the inflammatory cells, corneal edema characterized by opacity and neovascularization (Gupta et al., 2020). Currently, there is a lack of effective therapies to mitigate the impact of acrolein exposure, as molecular mechanisms underlying acrolein toxicity in the cornea are unknown.

The hCSF cultures were used to investigate the acrolein mechanism of action and to find out the target for acrolein toxicity. We first optimize the dose of acrolein in the hCSFs using cell viability assays. We found that acrolein showed a dose-dependent cell toxicity in hCSFs similar to that seen in other *in vitro* studies as reported in somatic cells of *Drosophila* and alveolar basal epithelial cells of human (Demir et al., 2013; Moghe et al., 2015; Zhang et al., 2018). The IC_{50} for acrolein was found to be 100 μM and was used in this study to investigate the cytotoxic effect of acrolein in hCSFs (Fig. 1).

Acrolein exposure causes damage to the cells and tissue using multiple mechanism of toxicity. Previously studied mechanisms showed that acrolein binds diectly to cellular components forming protein and DNA adducts. Alternatively, acrolein can indirectly initiate oxidative, mitochondrial, and ER stress (Chen et al., 2016; Moghe et al., 2015). Acrolein has been known to cause oxidative stress in the retinal, respiratory, renal, cardiovascular, and neural tissues (Conklin et al., 2017; DeJarnett et al., 2014; McDowell et al., 2018; Moghe et al., 2015; Shi et al., 2011). Similarly, we found that acrolein exposure significantly elevated levels of ROS and LPO (Fig. 2) with significantly decreased GSH levels (Fig. 3B) in the hCSFs.

GSH plays a vital role in the transport of amino acids and acts as a coenzyme to protect cells against the oxidative stress. Our biochemical data showed that the GSH was significantly compromised during acrolein-induced toxicity in hCSFs. The levels of GSH, in turn, regulate the activity of another family of antioxidant enzymes called glutathions peroxidases (GPxs). Glutathione peroxidases (GPXs) are important enzymes in the glutathioneascorbate cycle that play an important role in oxidative stress. Out of several GPxs, in this study, GPx4 has been studied due to it’s unique ability and nature to protect the lipid peroxides that intergared in the membrane. (Brigelius-Flohé and Maiorino, 2013; Yang et al., 2014). Also, GPx4 has been suggested to play an essential role in the oxidative homeostasis of the corneal tissue (Sakai et al., 2016; Uchida et al., 2017). We found that the expression of GPx4 was significantly decreased in the acrolein exposed hCSFs, suggesting a major breakdown in the GSH-GPx cellular metabolism in the corneal fibroblasts (Fig. 3C). To further prove that the adverse effects of acrolein in hCSFs were related to GSH homeostasis, we used buthionine sulfoximine (BSO), a selective and potent inhibitor of glutamyl cysteine synthetases that inhibits the glutathione synthesis (Haddad, 2000). We used cell viability assay to optimize the dose of BSO and found that 100 mM was found to be safe in hCSFs (Fig. 3A). It is interesting to note that the combined exposure of BSO and acrolein further potentiated the loss of GSH and GPx4 levels in hCSFs.

Next, we studied the role of acrolein toxicity in the mitochondrial function, which play a pivotal role in the regulation of ROS and GSH metabolism. The mitochondria contains an arsenal of antioxidants and detoxifying enzymes. Mitochondrial glutathione is the main

line of defense for the maintenance of the appropriate mitochondrial redox environment to avoid or repair oxidative modifications that may lead to mitochondrial dysfunction and cell death (Marí et al., 2009; Ribas et al., 2014; Zorova et al., 2018). We studied the changes in mitochondrial membrane potential ($\Delta\Psi m$), which are considered as the sensitive markers of cellular injury in acute exposures to toxins (National Academies of Sciences, 2015). Our data showed that acrolein exposure caused depolarization of mitochondria in hCSFs (Fig. 4). Also, the mitochondrial membrane potential regulates the level of antioxidative enzymes, and mitochondrial depolarization may be a protective reaction in response to acrolein induced oxidative stress unless accompanied with increased mitochondrial membrane permeability (Zorova et al., 2018). Acrolein increased the expression levels of BAD and BAX genes in the hCSFs suggesting increased mitochondrial membrane permeability and mitochondrial dysfunction (Fig. 4D & E). This may cause cytochrome C release and culminate in cell death. Acrolein exposure has been reported to induce DNA strand breaks in spleen lymphocytes (Yang et al., 1999), in neuronal cells (Huang et al., 2013), and in lung epithelial cells (Sun et al., 2014; Tirumalai et al., 2002). To further evaluate the impact of acrolein on cellular toxicity, TUNEL and caspase 3/7 activity assays were performed in hCSFs, and found that acrolein caused cell toxicity and triggered apoptosis via caspase 3/7 pathway (Fig. 5).

The biochemical changes in oxidative stress, mitochondrial membrane potential, and cytotoxicity data showed a critical role of glutathione availability in the acrolein induced cytotoxicity in hCSFs. Previous literature suggests that GSH is presently the most studied antioxidant due to its endogenous synthesis by the cells. GSH has multiple roles in cellular function, including antioxidant defense, detoxification of electrophilic xenobiotics, modulation of redox-regulated signal transduction, storage and transport of cysteine, regulation of cell proliferation, synthesis of deoxyribonucleotide synthesis, regulation of immune responses, and regulation of leukotriene and prostaglandin metabolism (Aquilano et al., 2014; Forman et al., 2009; Kerksick and Willoughby, 2005). In the cellular environment, the GSH also plays an important role in minimizing the lipid peroxidation of cellular membranes to regulate oxidative stress (Kerksick and Willoughby, 2005). In the eye, GSH is the most abundant biological antioxidant found in the mammalian tear fluid. It protects protein thiol groups by affording protection against ROS, is necessary for the function of several glutathione-dependent antioxidant enzymes that neutralize ROS, and is responsible for detoxification (Ganea and Harding, 2006; Umapathy et al., 2013). Recent studies on GSH turnover showed the direct envolvement of GSH in ocular surface protection and maintenance during oxidative stress triggered via chemicals (Chen et al., 2009). Since depletion of GSH led to the staggering toxic effects of acrolein in hCSFs, we used N-acetylcysteine (NAC), a well known precursor of glutathione metabolism to define the role of GSH in acrolein toxicity.

NAC is a commercially available, inexpensive, and clinically used cysteine analog in several medical conditions (Salamon et al., 2019). At the cellular level, the balance between oxidative and antioxidative index is essential for cellular function, DNA integrity, and signal transduction (Kerksick and Willoughby, 2005). From our dose-response study, we found that NAC up to 1 mM dose was safe in hCSFs to investigate the protective effects against acrolein toxicity (Fig. 6A). The phase-contrast live microscopy data showed that acrolein

exposure causes cellular toxicity in hCSFs, but NAC treatment mitigates and maintains cellular morphology in hCSFs (Fig. 6 B–E). We perfomed biochemical assays and found that NAC significantly reduced oxidative stress (ROS and LPO) and elevated the glutathione (GSH) levels in the acrolein exposed hCSFs (Fig. 7). The Mitotracker dye data also showed restoration of the mitochondrial membrane potential and substantiate the impact of GSH rescue in the acrolein-induced damage to hCSFs (Fig. 8). Futher, reduction in the caspase 3/7 activity in acrolein exposed cells confirmed the protective role of NAC treatment in hCSFs.

5. Conclusion

In summary, acrolein exposure increased oxidative stress, depleted glutathione levels, depolarized mitochondrial membrane, and activated caspase 3/7 to trigger cell death in hCSFs (Fig. 9). We found that reinstating the GSH levels with NAC treatment effectively mitigated acrolein toxicity, thus suggesting GSH as a potential target in hCSFs.

Acknowledgment

The authors thank Landon M. Keele for careful reading of the manuscript.

Funding

This work was primarily supported by the National Eye Institute, NIH, Bethesda, Maryland (5R21EY030233) Grant (R.R. M.); partially by a pilot grant (S.G.) from the Truman VA Medical Research Foundation, Columbia, Missouri; National Eye Institute, NIH, NEI, Bethesda, Maryland (5R21EY030234; 5R01EY017294; and 1R01EY030774) Grants (R.R.M.); the United States Veterans Health Affairs, Washington, DC, (1I01BX000357) Merit grant; and RCS award (R.R.M.).

Abbreviations:

ACR	acrolein
hCSFs	human corneal stromal fibroblasts
ROS	reactive oxygen species
GSH	glutathione
LPO	lipid peroxidation
NAC	N-acetyl cysteine
BSO	buthionine sulphoximine
CTL	non-exposed DMEM control
RFU	relative fluorescence unit
MTT	3-45-dimethylthiazol-2-yl)-2,5-diphenyltetrazolium bromide
DCHF-DA	dichlorodihydrofluorescin diacetates

References

Aquilano K, Baldelli S, Ciriolo MR, 2014. Glutathione: new roles in redox signaling for an old antioxidant. Front. Pharmacol. 5 196–196. [PubMed: 25206336]

Ashizawa A, Roney N, Taylor J, 2007. Toxicological Profile for Acrolein.

Brigelius-Flohé R, Maiorino M, 2013. Glutathione peroxidases. Biochim. Biophys. Acta BBA - Gen. Subj. 1830, 3289–3303 Cellular functions of glutathione.

Chen Y, Mehta G, Vasiliou V, 2009. Antioxidant defenses in the ocular surface. Ocul. Surf. 7, 176–185. [PubMed: 19948101]

Chen W-Y, Zhang J, Ghare S, Barve S, McClain C, Joshi-Barve S, 2016. Acrolein is a pathogenic mediator of alcoholic liver disease and the scavenger hydralazine is protective in mice. Cell. Mol. Gastroenterol. Hepatol. 2, 685–700. [PubMed: 28119953]

Claeson A-S, Lind N, 2016. Human exposure to acrolein: time-dependence and individual variation in eye irritation. Environ. Toxicol. Pharmacol. 45, 20–27. [PubMed: 27235799]

Conklin DJ, Haberzettl P, Jagatheesan G, Kong M, Hoyle GW, 2017. Role of TRPA1 in acute cardiopulmonary toxicity of inhaled acrolein. Toxicol. Appl. Pharmacol. 324, 61–72. [PubMed: 27592100]

Dachir S, Cohen M, Gutman H, Cohen L, Buch H, Kadar T, 2015. Acute and long-term ocular effects of acrolein vapor on the eyes and potential therapies. Cutan. Ocul. Toxicol. 34, 286–293. [PubMed: 25363068]

DeJarnett N, Conklin DJ, Riggs DW, Myers JA, O'Toole TE, Hamzeh I, Wagner S, Chugh A, Ramos KS, Srivastava S, Higdon D, Tollerud DJ, DeFilippis A, Becher C, Wyatt B, McCracken J, Abplanalp W, Rai SN, Ciszewski T, Xie Z, Yeager R, Prabhu SD, Bhatnagar A, 2014. Acrolein exposure is associated with increased cardiovascular disease risk. J. Am. Heart Assoc. 3 (4) doi:10.1161/JAHA.114.000934.

Demir E, Turna F, Kaya B, Creus A, Marcos R, 2013. Mutagenic/recombinogenic effects of four lipid peroxidation products in Drosophila. Food Chem. Toxicol. 53, 221–227. [PubMed: 23238235]

Exposures, C. on P.-T.A. for M.A. of A., Toxicology, C. on, Toxicology, B. on E.S. and, Sciences, B. on L., Studies, D. on E. and L., The National Academies of Sciences, E, 2015. Assays for Predicting Acute Toxicity. National Academies Press, US.

Forman HJ, Zhang H, Rinna A, 2009. Glutathione: overview of its protective roles, measurement, and biosynthesis. Mol. Aspects Med. 30, 1–12. [PubMed: 18796312]

Ganea E, Harding JJ, 2006. Glutathione-related enzymes and the eye. Curr. Eye Res. 31, 1–11. [PubMed: 16421014]

Ghilarducci DP, Tjeerdema RS, 1995. Fate and effects of acrolein. In: Ware GW (Ed.), Reviews of Environmental Contamination and Toxicology, Reviews of Environmental Contamination and Toxicology. Springer New York, New York, NY, pp. 95–146.

Gupta R, Buss DG, Mohan RR, Kanwar JR, Yarnall BW, Giuliano EA, 2011. Mitomycin C: a promising agent for the treatment of canine corneal scarring [electronic resource]. Vet. Ophthalmol. 14, 304–312. [PubMed: 21929607]

Gupta S, Rodier JT, Sharma A, Giuliano EA, Sinha PR, Hesemann NP, Ghosh A, Mohan RR, 2017. Targeted AAV5-Smad7 gene therapy inhibits corneal scarring in vivo. PLoS One 12, 1–18.

Gupta S, Fink MK, Ghosh A, Tripathi R, Sinha PR, Sharma A, Hesemann NP, Chaurasia SS, Giuliano EA, Mohan RR, 2018. Novel combination BMP7 and HGF gene therapy instigates selective myofibroblast apoptosis and reduces corneal haze in vivo. Invest. Ophthalmol. Vis. Sci. 59, 1045–1057. [PubMed: 29490341]

Gupta S, Fink MK, Martin LM, Sinha PR, Rodier JT, Sinha NR, Hesemann NP, Chaurasia SS, Mohan RR, 2020. A rabbit model for evaluating ocular damage from acrolein toxicity in vivo. Ann. N. Y. Acad. Sci. 1480 (1), 233–245. doi:10.1111/nyas.14514. [PubMed: 33067838]

Haddad J, 2000. L-buthionine-(S,R)-sulfoximine, an irreversible inhibitor of γ-glutamylcysteine synthetase, augments LPS-mediated proinflammatory cytokine biosynthesis: evidence for the implication of an IκB-α/NF-κB insensitive pathway. Eur. Cytokine Netw. 12, 614–624.

Huang Y-J, Jin M-H, Pi R-B, Zhang J-J, Ouyang Y, Chao X-J, Chen M-H, Liu P-Q, Yu J-C, Ramassamy C, Dou J, Chen X-H, Jiang Y-M, Qin J, 2013. Acrolein induces Alzheimer's disease-like pathologies in vitro and in vivo. Toxicol. Lett. 217, 184–191. [PubMed: 23296102]

Jia L, Liu Z, Sun L, Miller SS, Ames BN, Cotman CW, Liu J, 2007. Acrolein, a toxicant in cigarette smoke, causes oxidative damage and mitochondrial dysfunction in RPE cells: protection by (r)-α-Lipoic acid. Investig. Opthalmol. Vis. Sci. 48, 339.

Jia L, Zhang Z, Zhai L, Bai Y, 2009. Protective effect of lipoic acid against acrolein-induced cytotoxicity in IMR-90 human fibroblasts. J. Nutr. Sci. Vitaminol. (Tokyo) 55, 126–130. [PubMed: 19436138]

Kerksick C, Willoughby D, 2005. The antioxidant role of glutathione and N-AcetylCysteine supplements and exercise-induced oxidative stress. J. Int. Soc. Sports Nutr. 2, 38–44. [PubMed: 18500954]

Lim RR, Tan A, Liu Y-C, Barathi VA, Mohan RR, Mehta JS, Chaurasia SS, 2016. ITF2357 transactivates Id3 and regulate TGFβ/BMP7 signaling pathways to attenuate corneal fibrosis. Sci. Rep. 6 20841–20841. [PubMed: 26865052]

Marí M, Morales A, Colell A, García-Ruiz C, Fernández-Checa JC, 2009. Mitochondrial glutathione, a key survival antioxidant. Antioxid. Redox Signal. 11, 2685–2700. [PubMed: 19558212]

McDowell RE, Barabas P, Augustine J, Chevallier O, McCarron P, Chen M, McGeown JG, Curtis TM, 2018. Müller glial dysfunction during diabetic retinopathy in rats is reduced by the acrolein-scavenging drug, 2-hydrazino-4,6-dimethylpyrimidine. Diabetologia 61, 2654–2667. [PubMed: 30112688]

Moghe A, Ghare S, Lamoreau B, Mohammad M, Barve S, McClain C, Joshi-Barve S, 2015. Molecular mechanisms of acrolein toxicity: relevance to human disease. Toxicol. Sci. 143, 242–255. [PubMed: 25628402]

Ribas V, García-Ruiz C, Fernández-Checa JC, 2014. Glutathione and mitochondria. Front. Pharmacol. 5, 151. doi:10.3389/fphar.2014.00151. [PubMed: 25024695]

Rodier JT, Tripathi R, Fink MK, Sharma A, Korampally M, Gangopadhyay S, Giuliano EA, Sinha PR, Mohan RR, 2019. Linear Polyethylenimine-DNA nanoconstruct for corneal gene delivery. J. Ocul. Pharmacol. Ther. 35, 23–31. [PubMed: 30699061]

Sakai O, Uchida T, Imai H, Ueta T, 2016. Glutathione peroxidase 4 plays an important role in oxidative homeostasis and wound repair in corneal epithelial cells. FEBS Open Bio 6, 1238–1247.

Salamon S, Kramar B, Marolt TP, Poljšak B, Milisav I, 2019. Medical and dietary uses of N-Acetylcysteine. Antioxidants 8 (5),111. doi:10.3390/antiox8050111.

Shah H, Speen AM, Saunders C, Brooke EA, Nallasamy P, Zhu H, Li YR, Jia Z, 2015. Protection of HepG2 cells against acrolein toxicity by 2-cyano-3,12-dioxooleana-1,9-dien-28-imidazolide via glutathione-mediated mechanism. Exp. Biol. Med. 240, 1340–1351.

Sharma A, Rodier JT, Tandon A, Klibanov AM, Mohan RR, 2012. Attenuation of corneal myofibroblast development through nanoparticle-mediated soluble transforming growth factor-β type II receptor (sTGFβRII) gene transfer. Mol. Vis. 18, 2598–2607. [PubMed: 23112572]

Shi R, Rickett T, Sun W, 2011. Acrolein-mediated injury in nervous system trauma and diseases. Mol. Nutr. Food Res. 55, 1320–1331. [PubMed: 21823221]

Sun Y, Ito S, Nishio N, Tanaka Y, Chen N, Isobe K, 2014. Acrolein induced both pulmonary inflammation and the death of lung epithelial cells. Toxicol. Lett. 229, 384–392. [PubMed: 24999835]

Tirumalai R, Rajesh Kumar T, Mai KH, Biswal S, 2002. Acrolein causes transcriptional induction of phase II genes by activation of Nrf2 in human lung type II epithelial (A549) cells. Toxicol. Lett. 132, 27–36. [PubMed: 12084617]

Uchida T, Sakai O, Imai H, Ueta T, 2017. Role of glutathione peroxidase 4 in corneal endothelial cells. Curr. Eye Res. 42, 380–385. [PubMed: 27420751]

Umapathy A, Donaldson P, Lim J, 2013. Antioxidant delivery pathways in the anterior eye. Biomed Res. Int. 2013, 207250 doi:10.1155/2013/207250. [PubMed: 24187660]

Xiao B, Deng X, Zhou W, Tan E-K, 2016. Flow cytometry-based assessment of mitophagy using MitoTracker. Front. Cell. Neurosci. 10, 76. doi:10.3389/fncel.2016.00076. [PubMed: 27065339]

Yang Q, Hergenhahn M, Weninger A, Bartsch H,1999. Cigarette smoke induces direct DNA damage in the human B-lymphoid cell line Raji. Carcinogenesis 20, 1769–1775. [PubMed: 10469623]

Yang WS, SriRamaratnam R, Welsch ME, Shimada K, Skouta R, Viswanathan VS, Cheah JH, Clemons PA, Shamji AF,Clish CB, Brown LM, Girotti AW, Cornish VW, Schreiber SL, Stockwell BR, 2014. Regulation of ferroptotic cancer cell death by GPX4. Cell 156, 317–331. [PubMed: 24439385]

Zhang S, Chen H, Wang A, Liu Y, Hou H, Hu Q, 2018. Combined effects of coexposure to formaldehyde and acrolein mixtures on cytotoxicity and genotoxicity in vitro. Environ. Sci. Pollut. Res. Int. 25, 25306–25314. [PubMed: 29946839]

Zorova LD, Popkov VA, Plotnikov EY, Silachev DN, Pevzner IB, Jankauskas SS, Babenko VA, Zorov SD, Balakireva AV, Juhaszova M, Sollott SJ, Zorov DB, 2018. Mitochondrial membrane potential. Anal. Biochem. 552, 50–59. [PubMed: 28711444]

HIGHLIGHTS

- Acrolein exposure causes oxidative stress in human corneal stromal fibroblasts.
- Oxidative stress leads mitochondrial dysfunction and cause cell death after acrolein exposure.
- Glutathione can be a potential target to limit acrolein toxicity in human cornea.

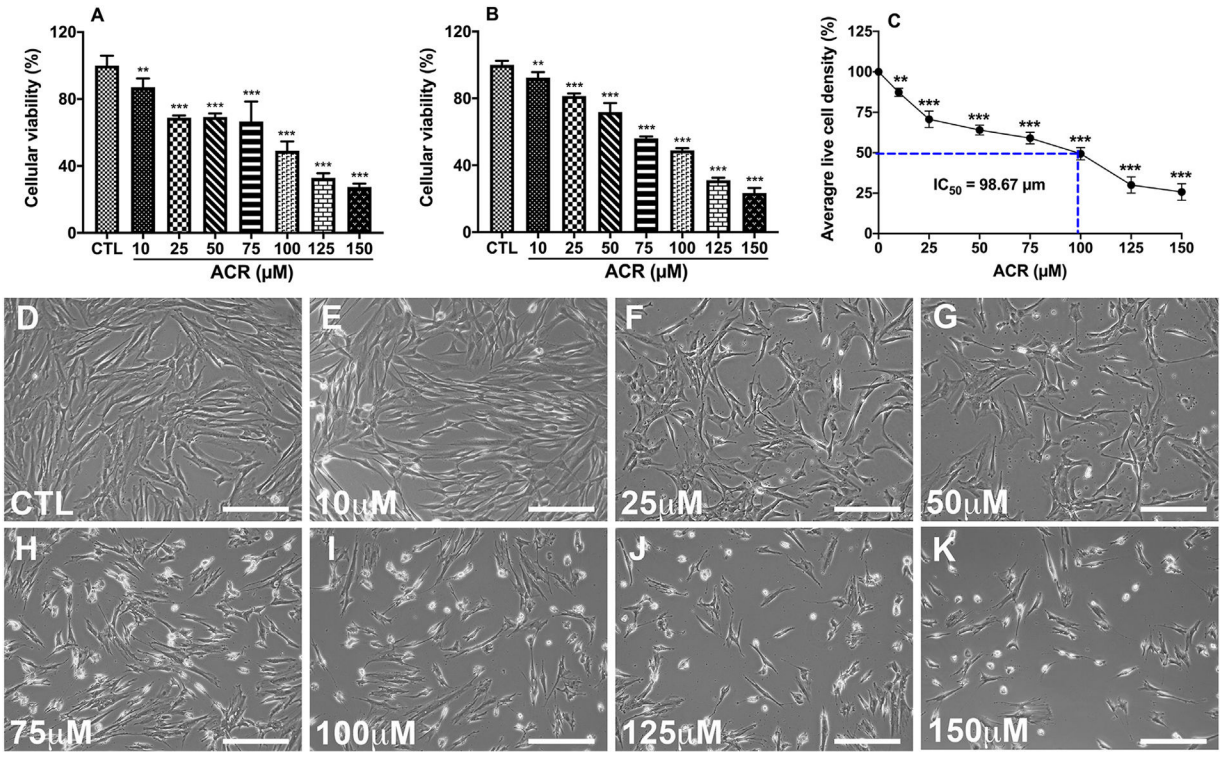

Fig. 1.

Cell viability assays showed the dose-dependent cytotoxicity of acrolein exposure in hCSFs. MTT cell proliferation assay (A) displayed a similar dose-response of cytotoxicity as observed with PrestoBlue Cell viability assay (B), and acrolein was found to have IC_{50} of 98.67 μm (C) in hCSFs at 4 h. Further, the phase-contrast live bio-microscopic images displayed the dose-dependent cellular cytotoxicity in hCSFs after acrolein exposure (D-K). All the experiments were independently performed three times using each sample in triplicates. The results were presented as mean ± SEM. The one-way analysis of variance (ANOVA) with Bonferroni post hoc test were used for statistical analysis. Scale bar = 100 μm and $^{**}p \leq 0.01$, $^{***}p \leq 0.001$.

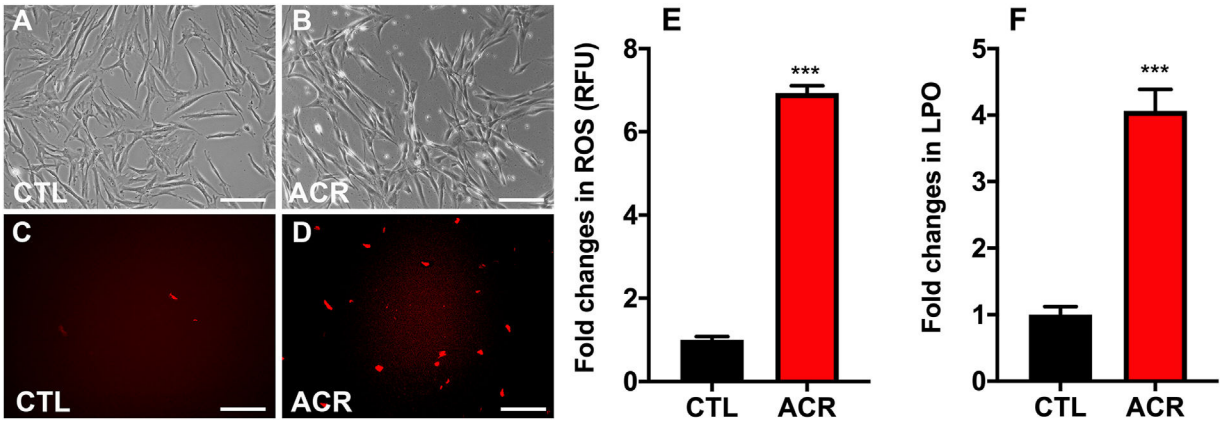

Fig. 2.

Acrolein exposure led to increased oxidative stress and lipid peroxides in hCSFs. Live cell bio-microscopy images depict the increased production of reactive oxygen species (ROS) in hCSFs as indicated by the intracellular DCF (2',7'-dichlorodihydrofluorescein) fluorescence in the acrolein exposed group (D) compared to the control group (C). The phase contrast images of hCSFs showed the morphological changes in acrolein −/+ groups, respectively (A, B). Quantitative analysis exhibited that acrolein (ACR) exposure significantly elevated the reactive oxygen species (ROS; E), and lipid hydrogen peroxide (LPO; F) levels compared to the control (CTL) group. All the experiments were independently performed three times using each sample in triplicates. The results were presented as mean ± SEM. The Student's *t*-test test were used for statistical analysis. Scale bar = 100 μm and ***$p \leq 0.001$.

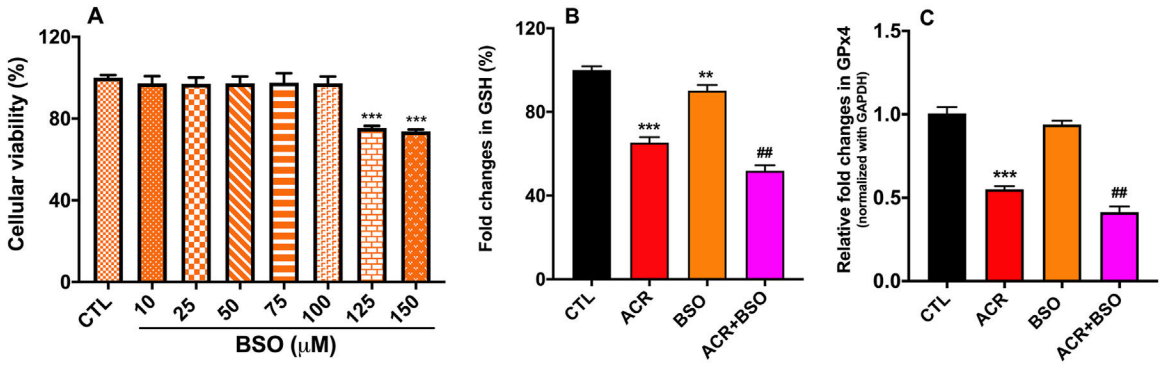

Fig. 3.

Acrolein exposure reduced glutathione (GSH) and glutathione peroxidase 4 (GPx4) levels in hCSFs. MTT cell viability assay showed the dose-dependent response of buthionine sulphoximine (BSO), a glutathione inhibitor (A) in hCSFs. Exposure to acrolein (ACR) significantly compromised GSH levels, which was further decreased in the presence of BSO (B). Quantitative RT-PCR data depicted that ACR exposure compromised the GPx4 level, which remained unchanged in the presence of BSO, (C). All the experiments were independently performed three times using each sample in triplicates. The results were presented as mean ± SEM. The one-way analysis of variance (ANOVA) with Bonferroni post hoc test were used for statistical analysis. $^{**}p \leq 0.01$, $^{***}p \leq 0.001$ compared to CTL group and $^{\#\#}p \leq 0.01$ compared to the ACR group.

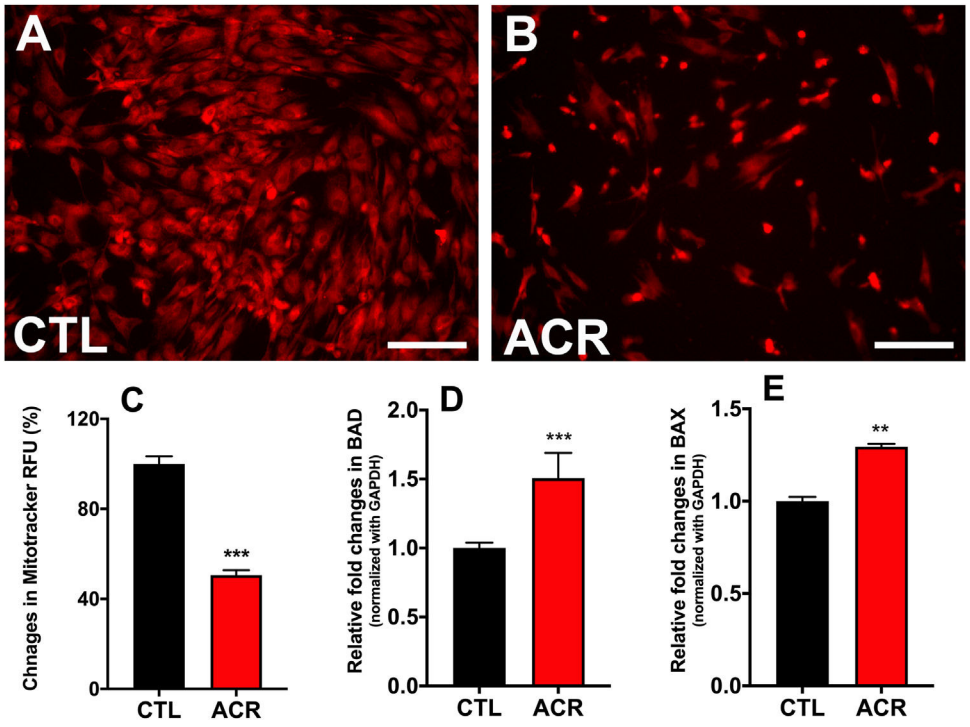

Fig. 4.

Acrolein exposure in hCSFs depolarized the mitochondria and increased membrane permeability. The live fluorescence bio-microscopy images obtained using MitoTracker Deep Red dye measuring mitochondrial membrane potential ($\Delta\Psi m$) in hCSFs showed that acrolein exposure caused lesser dye penetration (B) and hence increased mitochondrial dysfunction compared to the control (CTL) group (A). The quantification data showed ~50% reduction in the dye uptake (RFU) after acrolein exposure in hCSFs (C). Next, we measured the changes in the pro-apoptic genes BAD and BAX using qRT-PCR. We found that acrolein exposure (ACR) increased the BAD (D) and BAX (E) genes significantly (**$p \leq 0.01$) as compared control (CTL) group. All the experiments were independently performed three times using each sample in triplicates. The results were presented as mean ± SEM. The Student's *t*-test test was used for statistical analysis. Scale bar=100 μm.

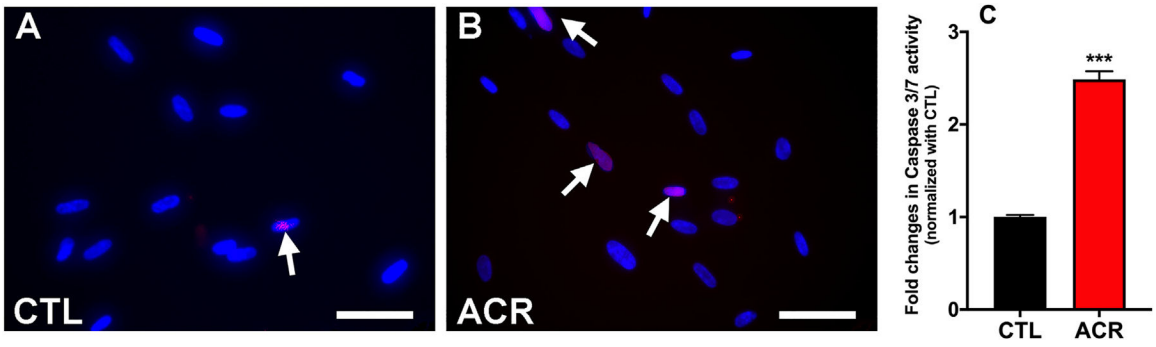

Fig. 5.

Acrolein exposure to hCSFs caused apoptosis and cell death. The TUNEL assay showed that acrolein exposure induced apoptosis as represented by the TUNEL + apoptotic cells (red color) in hCSFs (B) compared to the control group (A). Also, the caspase 3/7 activity assay displayed significantly increased levels in the acrolein exposed (ACR) hCSFs as compared to the control (CTL) group (C). All the experiments were independently performed three times using each sample in triplicates. The results were presented as mean ± SEM. The Student's *t*-test test were used for statistical analysis. Scale bar = 50 μm.

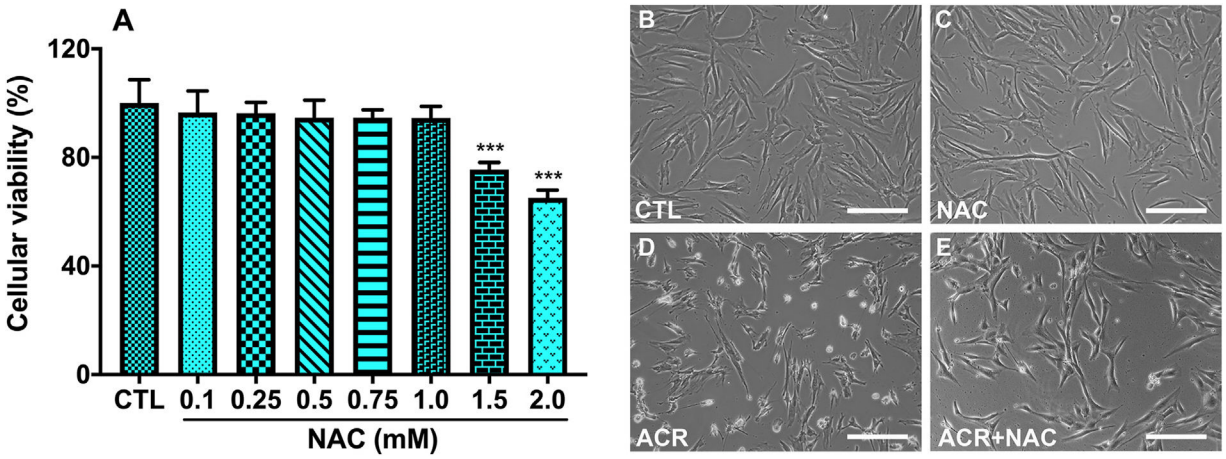

Fig. 6.

Cytoprotective effects of N-acetylcysteine (NAC) against acrolein exposure in hCSFs. Dose-dependent response of NAC using MTT assay was performed and dose upto 1 mM was found to be safe in hCSFs (A). The phase-contrast live bio-microscopic images showed that NAC at 1 mM concentration reduced (E) the adverse effects of acrolein exposure (ACR) on cellular viability in hCSFs (D). On the other hand, NAC treatment alone (C) showed similar cellular morphology to control group (B). All the experiments were independently performed three times using each sample in triplicates. The results were presented as mean ± SEM. The one-way analysis of variance (ANOVA) with Bonferroni post hoc test were used for statistical analysis. Scale bar = 100 μm.

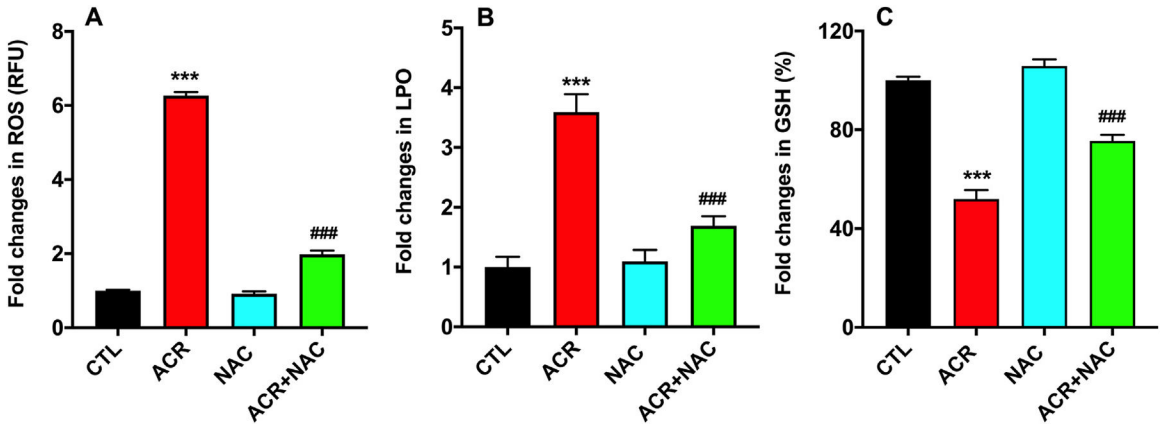

Fig. 7.

N-acetylcysteine (NAC) treatment to the acrolein exposed hCSFs showed significant reduction in the levels of reactive oxygen species (ROS; A), lipid peroxidation (LPO; B) in hCSFs. In addition, NAC treatment to the hCSF after acrolein exposure significantly increased GSH levels compared to the ACR group and rescued them to the near control (CTL) group (C). All the experiments were independently performed three times using each sample in triplicates. The results were presented as mean ± SEM. The one-way analysis of variance (ANOVA) with Bonferroni post hoc test were used for statistical analysis. ***$p \leq 0.001$, compare to the control group and $p \leq 0.001$ compared to the acrolein exposed (ACR) group.

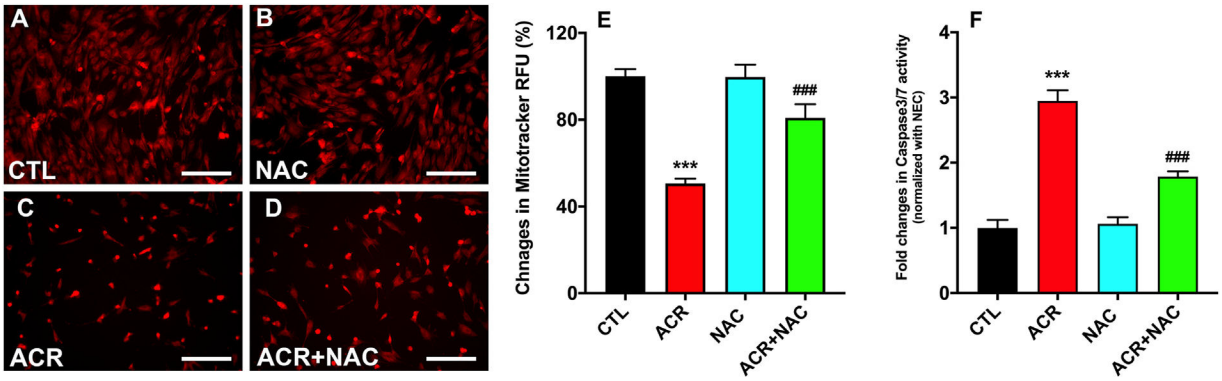

Fig. 8.

N-acetylcysteine (NAC) treatment to the acrolein exposed hCSFs displayed restoration of the mitochondrial membrane potential as measured by the MitoTracker Red dye (A-D). The quantification data suggested that NAC rescues the mitochondrial dysfunction after acrolein exposure significantly compared to the ACR group (E). Similarly, the caspase 3/7 activity was significantly decreased after NAC treatment in the acrolein exposure (ACR) group (F). All the experiments were independently performed three times using each sample in triplicates. $^{***}p \leq 0.001$ compared to the CTK group, and $^{\#\#\#}p \leq 0.001$ compared to the ACR group. All the experiments were independently performed three times using each sample in triplicates. The results were presented as mean ± SEM. The one-way analysis of variance (ANOVA) with Bonferroni post hoc test were used for statistical analysis. Scale bar=100 μm.

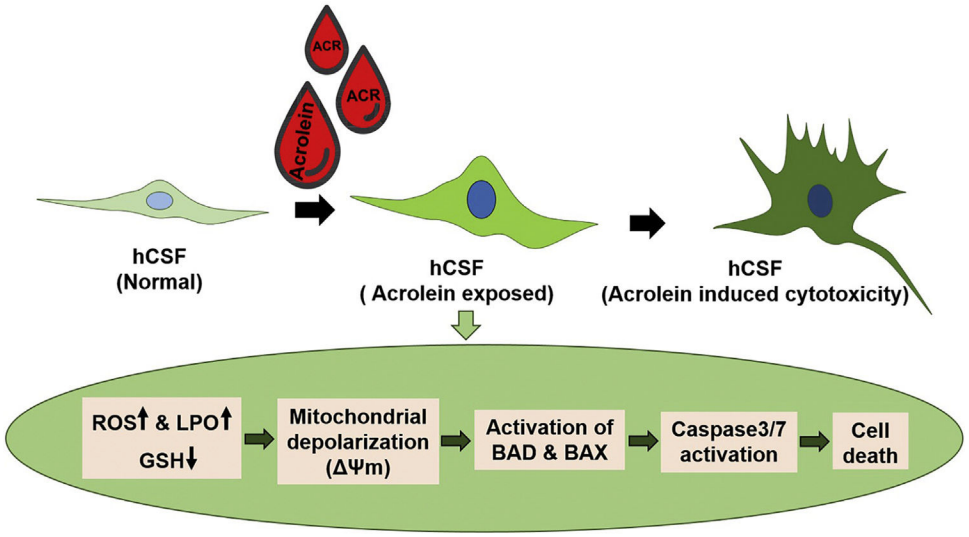

Fig. 9.

Schematic diagram describing the acrolein-induced biochemical changes in reactive oxygen species (ROS), lipid hyroperoxide (LPO), and glutathione (GSH) levels, which led to the mitochondrial dysfunction, and activation of caspase 3/7 signaling resulting in cell death in human corneal stromal fibroblasts (hCSFs).

Table 1

Sequence of primers used in the study.

Gene Name	Forward Primer (5’ 3’)	Reverse Primer (5’ 3’)	Accesion No.	Species	Amplicon size
BAD	GACGAGTTGTGGACTCCTTTA	CAAAGTTCCGATCCCACCAG	NM_004322.3	Human	123
BAX	GTCACTGAAGCGACTGATGT	CTTCTTCCAGATGGTGAGTGAG	NM_001291428.1	Human	128
GAPDH	GCCTCAAGATCATCAGCAATGCCT	TGTGGTCATGAGTCCTTCCACGAT	NM_002046.3	Human	104
GPx4	GGACACCGTCTCTCCACAGTT	GTCCTTCTCTATCACCAGGGG	NM_001039847.1	Human	94